Potential energy surface of monatomic liquids

Travis Sjostrom, Giulia De Lorenzi-Venneri, and Duane C. Wallace

Phys. Rev. B **98**, 054201 — Published 9 August 2018

DOI: 10.1103/PhysRevB.98.054201

Potential energy surface of monatomic liquids

Travis Sjostrom, Giulia De Lorenzi-Venneri, and Duane C. Wallace

Theoretical Division, Los Alamos National Laboratory, Los Alamos, New Mexico 87545

(Dated: July 23, 2018)

Abstract

In the last decade, significant progress has been made in the many-body Hamiltonian formulation of liquid dynamics theory. Earlier analysis of experimental data for a wide variety of elemental liquids had provided the reliable but qualitative description of the atomic motion: vibrations in a representative $3N$-dimensional potential energy valley, plus transits, in which atoms cross the intersections between these valleys. Recent comparisons of first-principles theory with experiment for several elemental liquids at melt revealed a highly accurate and versatile theory. In the present work, we report on an extensive quench study of the entire condensed-matter structure-energy distribution for a metallic Na MD system. With these results, all that was learned from experimental data is confirmed, refined in detail, and made more accurate. We show the entire structure-energy distribution, composed of widespread symmetrics and higher lying randoms; we show the increasing dominance of the randoms as N increases, until the symmetrics vanish completely; and we show the random distribution continue its spectacular narrowing as N continues to increase. This behavior certifies our early assignment of the random distribution to the liquid phase, and our prediction of macroscopic uniformity of the random structures. Procedures are discussed to identify and calibrate a single random structure to represent the liquid, and the role of the structure energy in liquid thermodynamics is described. A comparison with other liquid dynamics theories is observed in the Introduction, and the relation to the equation-of-state program is noted in the Conclusion.

I. INTRODUCTION

Much of what is known about condensed matter physics on the atomic and electronic level is expressed in Hamiltonian many-body theory. The basic technique is to first construct an approximate but tractable Hamiltonian for the system under study, then improve the theory by making an appropriate correction. While this formulation has provided excellent descriptions of the atomic dynamics in gas and crystal phases, it has not previously been successfully applied to liquid dynamics. Under the title of Vibration-Transit (V-T) theory, our research is developing this missing application of many-body theory.

V-T theory has been developed over many years, with improvements along the way. By now its major principles are settled. The atomic motion consists of two components, normal-mode vibrations in a representative $3N$-dimensional potential energy valley, plus transits, which carry atoms across the intersections between these valleys. The vibrational motion makes by far the dominant contribution to thermodynamic functions, and is treated by a first-principles tractable Hamiltonian. This dominant part of the theory is 100% predictive in all applications. The transit motion is treated by a two-parameter representation of a small portion of the many-body potential energy surface. This approximation produces the two key properties needed by a liquid dynamics theory: equilibrium melting upon increasing temperature from zero, and the concomitant appearance of self diffusion.

In two broad fields of application, namely thermodynamics and time correlation functions, V-T theory is now capable of producing highly accurate results when compared with experimental or MD data for elemental liquids. The thermodynamic functions studied include the internal energy and the entropy, and the zero-pressure liquid density and bulk modulus. The calculations are done with density functional theory, and also with interatomic potentials. These comparisons give us an unprecedented description of the atomic motion in the monatomic liquid. Evidence supports application of the same theory to liquid metallic alloys and molecular liquids. These thermodynamic studies will be referenced in the appropriate places in the following Sections.

In time correlation functions, V-T theory accurately accounts for MD data for the same Na system studied here[1,2]. The vibrational Hamiltonian is identical in both fields of application. The physical description of transits is also the same in both fields, but the transit calibration parameters differ. This is normal because equilibrium and non-equilibrium pro-

cesses measure different facets of the same atomic motion. We shall defer further comment on this work, since it is beyond our present scope.

From earlier times, and continuing today, liquid dynamics has a long history of theoretical study. Different formulations have been made, and much has been learned. The development of pseudopotential theory, and its application to the calculation of inter-ion potentials in nearly-free-electron (NFE) metals[3–5], provided a paradigm shift in liquid dynamics theory. The NFE metals provided then, as they still do, the most accurate and complete compilation of experimental data for elemental liquids. The natural inclination was to construct the theory of liquid thermodynamic functions in terms of inter-ion potentials and multi-ion spatial correlation functions[6,7]. This formulation was ultimately placed on a first-principles basis[8]. The work has been continued through a wide variety of applications in liquid dynamics theory[9,10]. Liquid state theories of the critical behavior were reviewed[11].

Another formulation, the 'phonon theory of liquid dynamics', was recently reviewed in extensive detail[12]. In this program, the atomic motion consists of two components, oscillatory and diffusive. The oscillatory contribution is Debye theory for N longitudinal and $2N$ transverse modes[13]. Diffusive motion is then accounted for by removing the lowest-frequency transverse modes, those with $\omega < \omega_F$, where $\omega_F(T)$ is the Frenkel frequency[14], of diffusive origin. A modification of the diffusive contribution has recently been presented[15,16]. The theory compares favorably with experimental data for constant volume specific heat of elemental and molecular liquids[17]. Moreover, the theory is applied to an extremely wide range of physical systems, including quantum liquids, glasses, and supercritical fluids.

There are two ways to compare V-T theory with the studies just mentioned. All are the same in their motivation to understand, and be able to calculate thermodynamic properties of liquids. On the other hand, their techniques for achieving this goal are as different as one can imagine, from the beginning. This is the normal theoretical response to a complex problem.

Condensed matter theory defines a structure as a stable quenched configuration, *i.e.* a configuration in which the force on every atom is zero and the system potential energy is a local minimum. For some years now, the atomic motional contribution to liquid thermodynamics in V-T theory has been resolved into three components: (a) The liquid-structure configuration and potential energy, which defines the classical groundstate; (b) the contribution from the vibrational normal modes in a $3N$-dimensional liquid valley; and (c) the

transit contribution. At this point we are preparing a detailed description of the theory and its application to thermodynamics, for each of the components (a), (b), and (c). Topic (a) is treated in the present work.

Our description of the liquid atomic motion is derived from several accurate analyses of experimental thermodynamic data for elemental liquids and crystals. This analytic research is briefly summarized over its 20 year timeline in Sec. II. Along with this analysis, we developed a description of the liquid potential energy surface (PES), referred to as the "Hypothesis", capable of rationalizing the experimental data.

Sec.III reports the results of an extensive quench study for liquid Na. We see the entire condensed-matter distribution of potential energy structures, the low-lying symmetric structures inhabited by the stable crystal and metastable amorphous solids, and the narrow high-lying random-structure distribution that dominates with increasing N, until the entire PES belongs to them. The random potential energy valleys are the domain of the liquid state.

In Sec.IV, the role of the random structure in the liquid groundstate is defined for classical mechanics. For the random structure distribution of Sec. III, the control of finite-N errors in Molecular Dynamics (MD) calculations is illustrated. Procedures required to identify and calibrate a single random structure for V-T theory are discussed.

The theory we are constructing is unique in its basic physical concepts. For further clarification, in Sec. V, points of progress in this study are summarized in terms of those underlying concepts. Accurate *ab initio* calculations of thermodynamic properties for several elemental liquids are mentioned. Beneficial application of V-T theory to equation-of-state work is discussed.

II. INFORMATION FROM EXPERIMENTAL DATA

The first episode in the development of the present liquid dynamics theory consisted of an extensive and long-running analysis of experimental thermodynamic data for elemental liquids. The analysis covers 41 elements for which highly accurate experimental data are available, distributed over 14 groups of the Periodic Table. The elements represent a wide range of electronic structures and interatomic potentials, including the rare gases, nearly-free-electron metals, s-p electron metals and transition metals. By finding common behavior

among such a physically diverse collection of elements, we are able to establish theory at a broadly general level. The primary experimental data set is the entropy S as function of temperature T at fixed volume V. The data are corrected from the volume at zero pressure to the volume of the liquid at melt, V_{lm}, by using additional thermodynamic data at $T > T_m$. The reason for this correction is that we want to extract the Hamiltonian parameters, such as system energy levels, and these parameters are constant, independent of T, for a liquid system at constant V. Here we shall summarize the foundational-level description of the liquid atomic motion, as derived from the early analysis of experimental data.

In a study of the melting of elements at high pressure P, Stishov discussed the changes of V and S upon melting at constant P, and also discussed anomalous melting curves, where T_m decreases with P[18]. In our study experimental melting entropy data, we corrected the crystal entropy to the volume V_{lm}, as mentioned above, and determined the entropy difference between liquid and crystal at T_m and V_{lm}, denoted as $\Delta S(V_{lm}, T_m)$[19]. This entropy difference showed two well-separated distributions. For 18 metallic elements with highly accurate data, the normal distribution has mean and standard deviation given by

$$\Delta S(V_{lm}, T_m) = (0.80 \pm 0.10) k_B. \tag{1}$$

For the elements studied the entropy of the liquid at melt is $S_m^l \approx 10 k_B$. Hence the mean $\Delta S(V_{lm}, T_m)$ is very small at around $0.08 S_m^l$, and the distribution width is extremely small at around $0.01 S_m^l$. The distribution is amazingly narrow for any physical parameter of a collection of liquids. In addition, 10 transition metals having less accurate data overall show a distribution mean close to that in Eq. 1, but with larger scatter (for the entire data set, see Table 22.1 of[20]).

The accurate melting analysis was done for 34 elements, of which six are anomalous[19]. For those six, $\Delta S(V_{lm}, T_m)$ ranges from $1.48 k_B$ for Sn to $3.85 k_B$ for Ge. These values are very large compared to the normal melting value, Eq. 1, and are widely spread. To rationalize this behavior, we observed that the electronic structure is unchanged (changed) between crystal and liquid in normal (anomalous) melting. This correlation significantly increases our understanding of the physics of melting. The bimodal ΔS distribution was not resolved in earlier studies because it is masked by the scatter of the experimental data at constant P ([18]; see also[7]).

Eventually, with the start of a Hamiltonian formulation of liquid dynamics, we directed

our analysis of experimental data toward sorting out the relation between the atomic motion and the PES. This sorting-out process is chronicled by the "Hypothesis", a developing list of characteristics of the PES that is indicated by experimental data.

It is generally considered that the condensed matter PES consists of a great many intersecting $3N$-dimensional potential energy valleys. Highly accurate evaluations of the atomic contribution to constant-volume specific heat were extracted from experimental data for elemental crystal and liquid phases at melt (Table I of[21]; Fig. 23.1 of[20]). The result is a uniform value of $3k_B$ for crystal and liquid alike, with small scatter. Exceptions are rationalized for Si[21] and Ar[20]. The result implies the atomic motion is nearly pure harmonic vibrations. This is understood for the crystal, for which the atoms vibrate in a single harmonic valley. To explain the same apparent behavior for the liquid, the supposition was made that the liquid potential energy valleys are uniform in their statistical mechanical properties (Paragraphs (a) and (b) of Sec.III, also Sec.VI, of[21]). The result is then rationalized by considering the liquid potential energy valleys to be harmonic.

In the same research report, the concept of transits was introduced[21]. However, the proper statistical mechanical treatment of transits was not developed until much later[22]. By then, the atomic motion was given two components, vibrations and transits, and statistical mechanical functions were composed accordingly. For example, the atomic motion contribution to entropy is $S_{vib} + S_{tr}$. Then, through an analysis of high-T experimental entropy for elemental liquids at V_{lm}, $S_{tr}(V_{lm}, T_m)$ was identified with $\Delta S(V_{lm}, T_m)$ of Eq. 1 (Sec.IIIA of[22]). This holds for normal and anomalous melters alike. The current Hypothesis statement follows.

A. Hypothesis

The entire complement of potential energy valleys falls in two classes, random and symmetric. The random valleys are maximally disordered within the constraints of boundary conditions and interatomic potentials. The maximal disorder implies that, among the total complement of structure energies, the randoms lie at the highest energies. Maximal disorder also implies that the random valleys are of overwhelming numerical superiority, and that they all have the same macroscopic statistical mechanical averages. The latter property is abbreviated by saying that the random valleys are 'macroscopically equivalent'. This equiv-

alence means that all random valleys have a common value of the structure potential, hence that the distribution of random-structure potential energies has zero width. This conclusion logically extends to all macroscopic statistical mechanical properties, and it implies that one can use a single random valley for liquid statistical mechanical calculations in a sufficiently large system. The characteristics just mentioned are evaluated in the thermodynamic limit, $N \to \infty$, and are subject to finite-N corrections.

In contrast, the symmetric valleys have some remnant of crystalline symmetry. All symmetric proportions are allowed, from a very minor content to single crystals. With exceptions of zero statistical weight, the symmetric structures lie in a broad distribution below the random distribution. The symmetrics are also relatively few in number, and make no contribution to statistical mechanics except at very small N, or very small T, well below T_m.

III. STRUCTURE-ENERGY DISTRIBUTION

An initial study of the N-dependence of the distribution of the Na structure potential, Φ_0, has been presented[23,24]. Similar computations are extended here, in order to reveal previously unresolved characteristics of the Φ_0 distribution. 1008 quenches are carried out from computer generated initial stochastic configurations at 8 values of N, ranging from 367 to 9883. Quenching from stochastic configurations is described in[23–25]. Here we make use of a well tested ion pair potential for Na[26,27] to determine the forces. We note though the technique has been used for Density Functional Theory (DFT) calculations of the liquid cold curves, *i.e.* the Φ_0 *vs* V curves, for Na and Cu[28].

Figure 1 shows the complete structure distribution for $N = 367$. The figure carries essential information on the statistical mechanics of a monatomic system, and illustrates in detail the Hypothesis stated at the end of Sec.II. The numerically-dominant high-lying narrow peak is the random distribution. The bcc crystal is the lowest-lying structure, and the bcc phase is stable at $T \leq T_m$. Between crystal and liquid lie the symmetric structures, characterized by varying degree of remnant crystalline symmetry. The symmetric valleys host single crystals, polycrystals, and amorphous solid states. Except for the stable crystal, the symmetric states are all metastable at all T. The entire random distribution is the domain of the liquid phase.

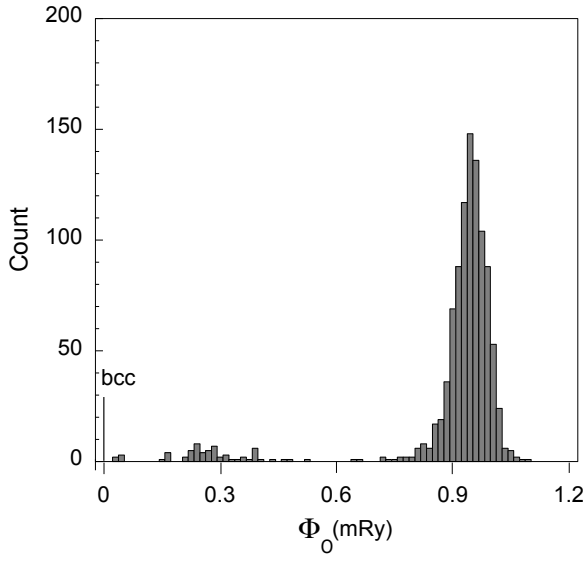

FIG. 1. Distribution of structure potentials Φ_0 at $N = 367$, from 1008 quenches. Φ_0 is measured from the bcc crystal. The dominant high-lying distribution consists of random structures, down to the first empty bin, and symmetric structures lie between bcc and the random distribution.

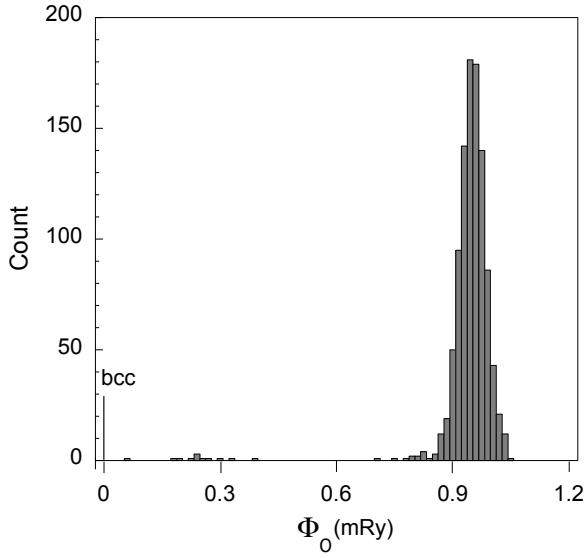

FIG. 2. Distribution of Φ_0 at $N = 500$. From Fig. 1, the random distribution narrows and the number of symmetrics decreases.

Two more structure distributions at increasing N are shown in Figs. 2 and 3. While the mean of the random distribution changes little with increasing N, its width decreases strongly. This property is encoded in the Hypothesis. From quantitative error estimates in Sec.IV, it is shown that the "sufficiently large system" is easily accessible to present day

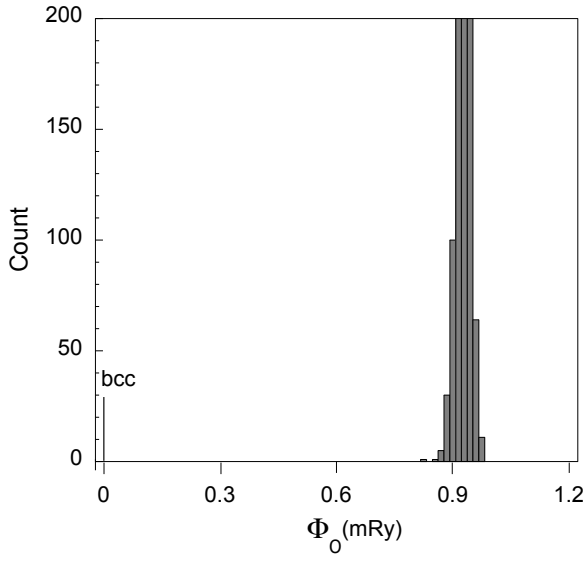

FIG. 3. Distribution of Φ_0 at $N = 1844$. From Fig. 2, the random distribution narrows further and only one symmetric is found.

MD calculations.

A visual of the narrowing of the random structure distributions from our lowest to highest N is shown in Fig. 4. This image directly shows the statistical concentration of random information as more samples are drawn (see the discussion of Fig. 6).

In contrast to the random structure distribution, the symmetric distribution remains broad as N increases, as shown in Figs. 1 and 2. However, while the numbers of random and symmetric valleys both increase dramatically as N increases, the numerical dominance of the randoms *also* increases dramatically, so that the number of symmetrics appearing in a fixed number of quenches soon vanishes. Starting with Fig. 1, the number of symmetric structures decreases in Fig. 2, and the last observed symmetric structure lies just below the narrowing random peak in Fig. 3. At larger N, no symmetric structures are found in 1008 quenches.

For theoretical work, we need to make a practical quantitative separation between symmetric and random structures. The symmetric character we have observed in quenched Na structures varies right across its allowed range, from a macroscopically distorted single crystal, to a nearly-random structure with one or two deformed nearest neighbor bcc configurations. We denote these structures respectively as global and local symmetrics. In Fig. 1, the broad symmetric distribution consists of global symmetrics; the excess wing on

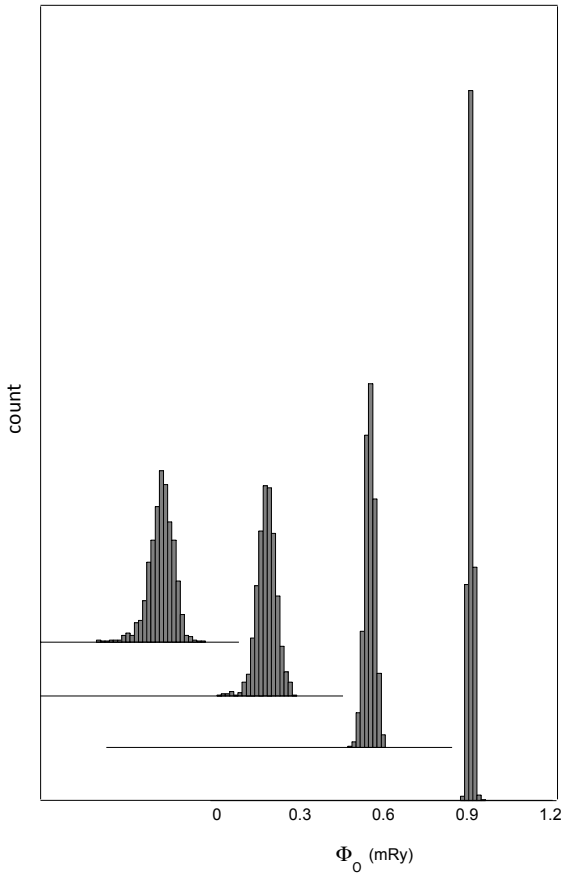

FIG. 4. Random Φ_0 distribution to a common scale from 1008 quenches at $N = 367, 500, 1844$ and 9883. The narrowing with increasing N reduces liquid statistical mechanics to a single random valley. All histograms are drawn to the same vertical and horizontal scales, and each histogram has the same total count, hence has the same area. The Φ_0 scale is shown for the far right histogram, and both scales for the first three histograms are marked in Figs. 1-3 respectively.

the low-energy side of the random distribution consists of a symmetry spread, and includes the local symmetrics. Our technique for separating symmetric and random structures is to divide them at the first empty histogram bin below the random peak. The technique is non-subjective. It has error, but only as a finite-N effect. Figures 1-3 show that the separation bin, the empty bin, moves up in potential energy as the distribution narrows. Hence the symmetric contamination of the random distribution goes to zero as N increases. Symmetric contamination is barely apparent in Fig. 3, and is not apparent in the larger-N distributions (see Fig. 4).

IV. CALIBRATION OF THE STRUCTURE THEORY

Let us denote a single random structure potential by Φ_0^r, and its average over the random distribution by $\langle\Phi_0^r\rangle$. The most accurate estimate we have for the liquid structure potential is $\langle\Phi_0^r\rangle$. However, each Φ_0^r corresponds to a specific configuration, in which the atomic equilibrium positions $\mathrm{R_K}$ are recorded, $K = 1, \ldots, N$. We need to keep this stable equilibrium configuration, as it is an essential part of the vibrational normal-mode theory, which in turn provides our entire vibrational formulation. But the structure configuration is lost in $\langle\Phi_0^r\rangle$. We therefore choose a structure whose potential is close to $\langle\Phi_0^r\rangle$, and denote it as the liquid structure with a superscript l. Φ_0^l is now the liquid structure potential, and carries with it a tabulation of the structure configuration. This information will be the starting point of our vibrational Hamiltonian. In that formulation, Φ_0^l is the classical groundstate energy, purely potential. For the quantum groundstate energy, the vibrational zero point energy is added to Φ_0^l.

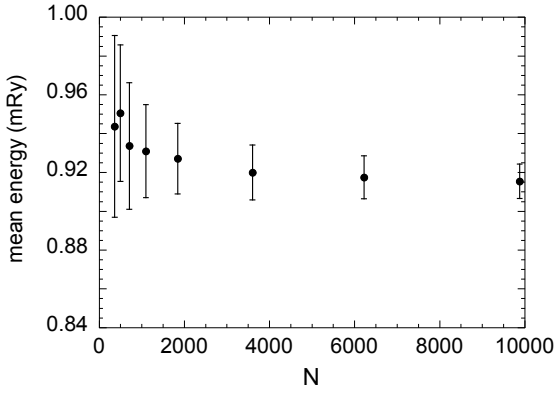

FIG. 5. Dots are the mean random-structure potential energy, $\langle\Phi_0^r\rangle$, graphed against N. The width bars are the Φ_0^r std dev at each N.

The internal energy in V-T theory, U_{VT}, has three major contributions, plus terms that are small at $T \gtrsim T_m$, as follows:

$$U_{VT}(V,T) = \Phi_0^l(V) + 3k_BT[1 + \ldots] + U_{tr}(V,T). \tag{2}$$

Here $3k_BT$ is the classical vibrational contribution, $[1+\ldots]$ represents the vibrational quantum corrections, and $U_{tr}(V,T)$ is the transit contribution. Notice we omit explicit consideration of the electronic thermal excitations in the present work. At $T \gtrsim T_m$, $3k_BT$ dominates

Eq. 2. Fig. 5 shows the mean and std dev of the Φ_0^r distributions *vs* N. The std dev measures scatter in the quench data. The scatter error at the largest N is 0.1% of $3k_BT_m$, and this percentage decreases as T increases. This error is insignificant for most applications. At $N = 500$, the scatter error is still only 1.0% of $3k_BT_m$. Two conclusions follow. (a) In MD calculations, only a modest N is required to reduce the Φ_0^r scatter error to a negligible level. (b) The first two terms on the right side of Eq. 2 have only numerical error; formal theoretical error is all contained in U_{tr}, and U_{tr} is small, being $\lesssim 0.1(3k_BT)$. Hence a simple approximate transit theory will in general be accurate enough. This condition is a benefit of the many-body Hamiltonian formulation.

Figure 6 shows the Φ_0^r std dev on a log-log graph, and its straight line fit. The graph reveals the operation of the central limit theorem, as follows. For an N-atom structure, let us define the single atom potential as $\phi_K, K = 1, \ldots, N$, and set $\Phi_0 = N^{-1}\sum_K \phi_K$. The key assumption of the central limit theorem is that the ϕ_K are randomly drawn from a fixed distribution, for every N. Then the theorem states that the Φ_0 distribution is proportional to $\exp(-N\Phi_0^2/2\sigma^2)$, with variance σ^2/N, σ =constant. This rationalization is justified by Fig. 6, because the std dev is found proportional to $N^{-\alpha}$, where $\alpha = 0.489$. α lies close enough to 0.5 to invoke the theorem. The practical significance of Fig. 6 is that it allows us to estimate computational error as function of N. The theoretical significance of Fig. 6 is its implication that the std dev goes to zero as N goes to infinity. This was assumed in the Hypothesis, in order to establish macroscopic uniformity of the random valleys (Sec.II).

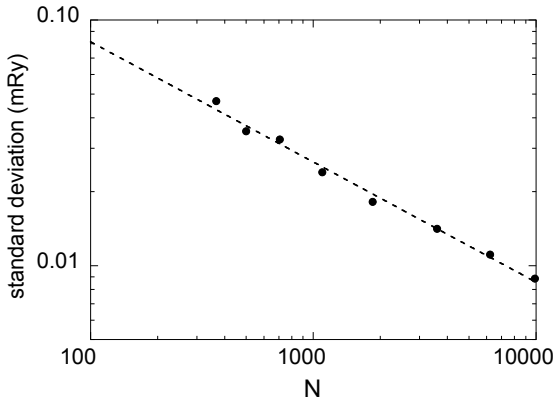

FIG. 6. Dots are the Φ_0^r std dev at each N, graphed against N on a log-log scale. Dashed straight line is a fit to the dots, and has slope -0.489.

We shall now discuss the procedures required to identify and calibrate a single liquid struc-

ture. We first consider normal melting elements, and work at fixed volume. Na is known to be NFE, in bcc and liquid phases. We verified this as a check on our DFT calculations by comparing the electronic density of states (DOS) for bcc and random structures. To search for random structures, one begins with a set of quenches, say 10, at fixed V and N. The quenched Φ_0^r should lie in a distribution above the stable crystal Φ_0^c by very approximately $k_B T_m$, and of width small compared to $k_B T_m$. Any apparent symmetrics are to be removed from the random distribution. Suspicious results are to be checked with additional independent quenches. It is always a good idea to do some testing of quenched structures. Several sensitive tests are illustrated in[29].

An alternative procedure works when V is to be varied. For Na and Cu, from one DFT quench at each of a set of volumes, the Φ_0^r *vs* V points lie on a smooth curve with very little scatter[28]. This also demonstrates a narrow Φ_0^r distribution. At this point, the quenched structures may all be designated liquid structures, and each structure configuration may be used to calibrate Φ_0^l and the vibrational normal mode theory.

The situation with anomalous melting can present a problem when theoretical calculations are done by DFT. For example, α-Ga is a partially covalent crystal, which melts to an NFE liquid. The problem is that quenches from the liquid can arrive at structures that are correct amorphous solids, but do not have the liquid electronic structure. This does not happen in Ga. For verification, we compared several definitive theoretical quantities from a set of quenched structures with the same quantities at the crystal structure. The quantities include the electronic DOS and the vibrational DOS (see Supplemental Material for[29]. It was verified in detail that the quenched structures are appropriate liquid structures.

However, the problem *does* appear in Si and Ge, the two most anomalous melters. DFT quenches from the NFE liquid arrive at structures with distorted covalent bonding, representative of the real amorphous solid[30]. The problem is not fatal, but is beyond the scope of our discussion.

V. DISCUSSION AND CONCLUSION

For many years, our goal has been to construct a Hamiltonian formulation of monatomic liquid dynamics. This goal requires only a single construction: A tractable approximate many-body potential energy function. From the early years, mentioned in Sec. II, we did

not think in terms of the general potential energy function $\Phi(\mathrm{r}_1, \ldots, \mathrm{r}_\mathrm{N})$, which depends on the instantaneous positions r_K of the atoms. Rather, we started with the conventional description of the many-atom PES as a collection of intersecting $3N$-dimensional potential valleys. We then analyzed experimental thermodynamic data for a collection of elemental liquids, to see what could be discovered about the macroscopic physical character of these potential energy valleys. This quest is minimally outlined in Sec.II. The information obtained from experimental data is primarily about the atomic motion. In all cases, it has eventually been possible to assign the information to vibrations or transits (Sec.II). The vibrations and transits then imply information about the underlying potential energy valleys, and this information is compiled in the Hypothesis (Sec.II). The Hypothesis is the template for the tractable many-body potential energy. Its variables are not the atomic positions, but are the $3N$-dimensional intersecting harmonic potential energy surfaces.

The study of quenched structures in Sec.III provides direct information about the potential energy valleys, as follows.

1. The study measures the complete condensed matter structure distribution and its N-dependence, for a physically realistic interatomic potential for Na at the volume of the liquid at melt. The result stands alone as an MD observation of the many-body PES.

2. The result verifies the Hypothesis accurately and in detail. In 8064 quenches, not one structure fails to follow the description at the end of Sec.II. Because the Hypothesis is based on experimental data from elemental liquids covering a broad range of bonding types, we expect the quench study of Sec.III to represent elements across a large portion of the Periodic Table.

3. Our primary interest is the liquid state. However, seeing the entire potential surface helps to clarify the liquid domain *and* its boundary. By convention, condensed matter physics identifies a phase by its structure. For example, bcc Na is a material phase, and its definition applies at all (V, T), whether the phase is stable or metastable. In this convention, we identify the liquid domain as the random valley distribution, for all (V, T).

Sec.IV begins the calibration of V-T theory. To keep the logic clear, we shall define exactly what is to be calibrated, though it transcends what is calibrated here. Let us define the V-T

potential $\Phi_{VT}(V)$, a tractable approximation to the potential recorded in the Hypothesis. $\Phi_{VT}(V)$ has three components: the liquid structure potential $\Phi_0^l(V)$; the harmonic potential $\Phi_{vib}(V)$, defined at the structure and extended to infinity; and correction to the extended harmonic potential to account for the intervalley intersections, denoted $\Phi_{tr}(V)$. Calibration of $\Phi_0^l(V)$ is described in Sec.IV. Notes are presented on how to identify and calibrate a single liquid valley. Ultimately, a data base on liquid calibration parameters will greatly enhance the general capability of calculating liquid properties. The corresponding much simpler data base for crystals is widely used. In this respect, an attractive property of V-T theory is that calibration of the liquid parameters at one volume enables calculation of thermodynamic properties at all temperatures, for that volume. This is another benefit of the many-body Hamiltonian formulation.

The present theoretical development is directly applicable to equation-of-state calculations. The thermodynamic equations for internal energy and entropy are written in[28,29]. In these references, structural and vibrational parameters are calculated from first-principles DFT. The transit contribution is from[31]. Calculations for Na and Cu as function of volume include the structure potential, pressure, bulk modulus, and the set of vibrational frequencies[28]. Data compared with experiment at T_m include the zero-pressure volume, the energy, entropy, and bulk modulus. The overall accuracy is phenomenal, being strictly as good as is lattice dynamics for the crystal (Table V in[28]). Calculations for crystal and liquid Ga at melt conditions allowed us for the first time to separate the normal and anomalous contributions to the melting process. Results for the liquid are again as accurate as for the crystal, and the thermodynamic changes across melting are very accurate (Tables II and IV of[29]).

Further V-T theory is well suited to be applied in general equation-of-state (EOS) modeling. EOS models are needed to provide thermodynamic materials properties over broad ranges of temperature and pressure for various hydrodynamic simulations including planetary modeling and shock physics simulations. Here the standard practice is to separate the total energy into three terms[32]

$$E = E_0 + E_i + E_e \,, \tag{3}$$

where E_0 is the cold curve or zero temperature compression curve, E_i is the thermal energy from the ions, and E_e is the thermal energy due to the electrons. In a multiphase approach this decomposition is done for each phase including the liquid, and then the phase boundaries

are determined by examining the Gibbs free energy[33–35]. The cold curve for the liquid is modeled in the same manner as the solid. That is using some sort of compression model above ambient density, *i.e.* Murnaghan EOS, and connecting to a gas model below such as a Lennard-Jones or Van der Waals EOS. This liquid cold curve is generally regarded as an abstraction and modeling convenience, and is often determined by extrapolating isotherms generated from above melt temperature *ab initio* calculation, or even just using the crystal cold curve. In contrast V-T theory provides a clear definition for what the cold curve of a liquid physically is and provides the EOS model contribution as $E_0 = \Phi_0^l$. This connection is a main point of this paper. The theory also provides the ion contribution to the energy E_i, or atomic motional energy, which is due to the vibrational plus transit potentials, $\Phi_{vib} + \Phi_{tr}$.

Current EOS modeling for the liquid is often based on solid-like Debye models near melt and interpolation to ideal gas like behavior at high temperatures[36,37]. Other approaches include perturbation theory approaches[38–41], usually of hard spheres, or semi-empirical parameterizing of Van der Waals type equations of state[33,42] which attempt to extend description to the liquid state. The advantage of V-T theory is in providing accurate thermodynamics for the EOS from melt up to temperatures of about $5T_{melt}$ above which one can connect to higher temperature models.

ACKNOWLEDGMENTS

We would like to thank Sven Rudin and Brad Clements for helpful and encouraging discussions. This work was performed under the auspices of Los Alamos National Laboratory, which is operated by Los Alamos National Security, LLC, for the National Nuclear Security Administration of the U.S. Department of Energy under Contract No. DE-AC52-06NA25396

---

[1] D. C. Wallace, G. De Lorenzi-Venneri, and E. D. Chisolm, Journal of Physics: Condensed Matter **28**, 185101 (2016).

[2] D. C. Wallace, E. D. Chisolm, and G. De Lorenzi-Venneri, Journal of Physics: Condensed Matter **29**, 055101 (2017).

[3] N. W. Ashcroft, Phys. Lett. **23**, 48 (1966).

[4] N. W. Ashcroft and D. C. Langreth, Phys. Rev. **155**, 682 (1967).

[5] W. A. Harrison, *Pseudopotentials in the Theory of Metals* (W. A. Benjamin, New York, 1966).

[6] P. A. Egelstaff, *An Introduction to the Liquid State* (Academic Press, New York, 1967).

[7] T. E. Faber, *Introduction to the Theory of Liquid Metals* (Cambridge University Press, Cambridge, 1972).

[8] N. W. Ashcroft and D. Stroud, in *Solid State Physics*, edited by H. Ehrenreich, F. Seitz, and D. Turnbull (Academic, New York, 1969), vol. 33, p. 1.

[9] N. H. March, *Liquid Metals* (Cambridge University Press, Cambridge, 1990).

[10] N. H. March and M. P. Tosi, *Introduction to Liquid State Physics* (World Scientific, New Jersey, 2002).

[11] A. Parola and L. Reatto, Advances in Physics **44**, 211 (1995).

[12] K. Trachenko and V. V. Brazhkin, Rep. Progr. Phys. **79**, 016502 (2016).

[13] K. Trachenko, Phys. Rev. B **78**, 104201 (2008).

[14] K. Trachenko and V. V. Brazhkin, Ann. Phys. **347**, 92 (2014).

[15] C. Yang, M. T. Dove, V. V. Brazhkin, and K. Trachenko, Phys. Rev. Lett. **118**, 215502 (2017).

[16] Y. D. Fomin, V. N. Ryzhov, E. N. Tsiok, J. E. Proctor, C. Prescher, V. B. Prakapenka, K. Trachenko, and V. V. Brazhkin, Journal of Physics: Condensed Matter **30**, 134003 (2018).

[17] D. Bolmatov, V. V. Brazhkin, and K. Trachenko, Sci. Rep. **2**, 421 (2012).

[18] S. M. Stishov, Sov. Phys.Usp. **11**, 816 (1969).

[19] D. C. Wallace, Proc. R. Soc. London, Ser. A **433**, 615 (1991).

[20] D. C. Wallace, *Statistical Physics of Crystals and Liquids* (World Scientific, New Jersey, 2002).

[21] D. C. Wallace, Phys. Rev. E **56**, 4179 (1997).

[22] D. C. Wallace, E. D. Chisolm, and N. Bock, Phys. Rev. E **79**, 051201 (2009).

[23] E. Holmström, N. Bock, T. Peery, R. Lizárraga, G. De Lorenzi-Venneri, E. D. Chisolm, and D. C. Wallace, Phys. Rev. E **80**, 051111 (2009).

[24] E. Holmström, N. Bock, T. Peery, E. Chisolm, R. Lizárraga, G. De Lorenzi-Venneri, and D. Wallace, Phys. Rev. B **82**, 024203 (2010).

[25] N. Bock, T. Peery, E. D. Chisolm, G. De Lorenzi-Venneri, D. C. Wallace, E. Holmström, and R. Lizárraga (2009), URL `http://meetings.aps.org/link/BAPS.2008.Mar.J9.4`.

[26] D. C. Wallace, Phys. Rev. **176**, 832 (1968).

[27] D. C. Wallace and B. E. Clements, Phys. Rev. E **59**, 2942 (1999).

[28] N. Bock, E. Holmström, T. B. Peery, R. Lizárraga, E. D. Chisolm, G. De Lorenzi-Venneri, and

D. C. Wallace, Phys. Rev. B **82**, 144101 (2010).

[29] S. P. Rudin, N. Bock, and D. C. Wallace, Phys. Rev. B **90**, 174109 (2014).

[30] S. Rudin (2018), private communication.

[31] D. C. Wallace, E. D. Chisolm, N. Bock, and G. De Lorenzi-Venneri, Phys. Rev. E **81**, 041201 (2010).

[32] S. P. Lyons and J. D. Johnson, Los Alamos Technical Report pp. LA–UR–92–3407 (1992).

[33] A. B. Medvedev, Combust Explos Shock Waves **50** (2014).

[34] G. A. Cox and M. A. Christie, Journal of Physics: Condensed Matter **27**, 405201 (2015).

[35] T. Sjostrom, S. Crockett, and S. Rudin, Phys. Rev. B **94**, 144101 (2016).

[36] J. D. Johnson, High Pressure Research **6**, 277 (1991).

[37] E. D. Chisolm, S. D. Crockett, and D. C. Wallace, Phys. Rev. B **68**, 104103 (2003).

[38] G. I. Kerley, J. Chem. Phys. **73**, 469 (1980).

[39] G. I. Kerley, J. Chem. Phys. **73**, 478 (1980).

[40] G. I. Kerley, J. Chem. Phys. **73**, 487 (1980).

[41] M. Ross, J. Chem. Phys. **71**, 1567 (1979).

[42] W. Zhong, C. Xiao, and Y. Zhu, Physica A: Statistical Mechanics and its Applications **471**, 295 (2017).